Review and Analysis of Molecular Simulations of Methane, Hydrogen, and Acetylene Storage in Metal-Organic Frameworks

Supporting Information

Rachel B. Getman[1], Youn-Sang Bae, Christopher E. Wilmer and Randall Q. Snurr[2]
Department of Chemical and Biological Engineering, Northwestern University, Evanston, IL 60208

October 6, 2011

This supporting information discusses the following:

1. Interaction models for H_2 with Li-doped and Li-alkoxide-functionalized IRMOF-8
2. Details of GCMC simulations
3. Reviews of simulated vs. experimental adsorption results for CH_4 and H_2 in MOFs.

S1. Interaction Models for H_2 with Li-Doped and Li-Alkoxide-Functionalized Variants of IRMOF-8

In section 5.3.2 of the main text, results are compared for simulations that use different model choices for hydrogen adsorption in Li-doped and Li-alkoxide-functionalized MOFs. Details of those simulations are provided here.

S1.1 H_2 Interactions with C, H, O, Zn, and H_2

H_2 interactions with framework C, H, O (excluding O in the alkoxide groups), and Zn atoms were calculated using Lennard-Jones potentials. Framework atom parameters were taken from the DREIDING force field.[1] Lennard-Jones Parameters for H_2 were taken from empirical data based on the second virial coefficient.[2] Each H_2 molecule was treated as a single sphere. Cross-

[1] Present address: Department of Chemical and Biomolecular Engineering, Clemson University, Clemson, SC 29634
[2] Corresponding author

term H_2/MOF parameters were obtained using the Lorentz-Berthelot mixing rules and are provided in Table S1. H_2/H_2 interactions were also computed using a Lennard-Jones potential, treating each H_2 molecule as a single sphere. All Lennard-Jones interactions were calculated out to a cut-off distance of 12 Å. This interaction model has been previously shown to reproduce experimental isotherms in un-doped, unfunctionalized MOFs very well.[3]

Table S1. Lennard-Jones parameters used to describe H_2/H_2 and H_2/framework atom interactions.

X	$\sigma_{H2\text{-}X}$ **(Å)**	$\varepsilon_{H2\text{-}X}/k_B$ **(K)**
Zn	3.499	31.884
C	3.214	41.910
H	2.90	16.76
O	2.994	42.054
H_2	2.958	36.700

S1.2 H_2 Interactions with Li and Li Alkoxide Groups

H_2 interactions with Li (doped MOFs) and Li alkoxide (functionalized MOFs) were calculated using Morse (doped MOFs) and Morse plus Coulomb potentials (functionalized MOFs.) Morse parameters were obtained from *ab initio* results (the parameterization procedures and final sets of parameters are given below.) Both H nuclei in the H_2 molecule were treated as Morse sites in these calculations. Partial charges in the alkoxide groups in functionalized MOFs were taken from *ab initio* calculations. The full procedure for obtaining these charges is described in depth in the Supporting Information by Getman et al.[4] For simulations on functionalized MOFs, partial charges along the H_2 axis were taken from the Darkrim-Levesque model,[5] which places charges of +0.468 at the H nuclei and a charge of −0.936 at the center of mass in order to simulate the quadrupole. Coulomb interactions were only calculated for the H_2/alkoxide O and H_2/alkoxide

Li interactions. All other charge-quadrupole, quadrupole-quadrupole, and other Coulomb effects were neglected in our simulations.

S1.3 H_2/Li and H_2/Li Alkoxide Morse Parameters

In this review, we calculated H_2 adsorption isotherms in Li-doped IRMOF-8 and Li-alkoxide-functionalized IRMOF-8. We calculated isotherms in Li-doped IRMOF-8 using three different sets of interaction parameters for H_2/Li. Two of these were developed in this work using two different Li^+ site models and the other was taken from Deng *et al.*[6] All force fields developed in this work were parameterized by fitting a pair potential to the electronic binding energies for H_2 adsorbed in a variety of configurations surrounding the Li^+ site,

$$\Delta E^{bind}(r) = E^{elec}_{\mathrm{Li^+-H_2}}(r) - E^{elec}_{\mathrm{Li^+}} - E^{elec}_{\mathrm{H_2}} \qquad \text{(Eq. S1)}$$

where 'Li^+' broadly describes the model containing the open Li^+ site. ΔE^{bind} values for the first set were calculated with MP2/6-311+G** between H_2 and a bare Li^+ cation and fit to a Morse potential

$$\mathcal{V}_{ij} = D_{ij}\left[\mathrm{e}^{\alpha_{ij}\left(1-r_{ij}/r^*_{ij}\right)} - 2\mathrm{e}^{\left(\alpha_{ij}/2\right)\left(1-r_{ij}/r^*_{ij}\right)}\right] \qquad \text{(Eq. S2)}$$

Note that this H_2/Li^+ system has a net charge of +1 in the quantum calculations. However all species were considered to be neutral in the pair potentials and GCMC calculations, i.e. the

charge/quadropole interactions were implicitly incorporated into the Morse potential instead of added as separate terms.

For the second parameter set, we used a similar procedure, this time using potential energies calculated between H_2 and a $Li^+(C_{10}H_8)^-$ model at the same level of theory. Note that Li in this system adopts a partial positive charge and $C_{10}H_8$ adopts the opposite charge, but the system as a whole is charge neutral. Here we only developed parameters to describe the H_2/Li^+ interaction, and H_2 interactions with all other atoms were simulated using the conventional force field models described above.

The third parameter set was taken from Deng *et al.*[6] All parameters are provided in Table S2.

We used two different interaction models to simulate H_2 adsorption in Li-alkoxide-functionalized IRMOF-8. The first set we took directly from our previous work,[4] which fit ΔE^{bind} between H_2 and Li alkoxide benzene models calculated at the MP2/6-311+G** level of theory to a Morse + Coulomb potential

$$\mathcal{V}_{ij} = -D_{ij}\left[1-\left(1-\mathrm{e}^{-\alpha_{ij}\left(r_{oj}-r_{ij}^{*}\right)}\right)^2\right]+\frac{q_i q_j}{4\pi\epsilon_0 r_{ij}} \qquad \text{(Eq. S3)}$$

The second set are Lennard-Jones parameters taken from Klontzas *et al.*[7] The Lennard-Jones equation is

$$\mathcal{V}_{ij} = 4\varepsilon_{ij}\left[\left(\frac{\sigma_{ij}}{r_{ij}}\right)^{12} - \left(\frac{\sigma_{ij}}{r_{ij}}\right)^{6}\right] \qquad \text{(Eq. S4)}$$

All parameters are provided in Table S2.

Table S2. Interaction parameters for H_2/Li (doped MOFs) and H_2/alkoxide O and H_2/alkoxide Li (functionalized MOFs) developed using different methods.

Li-Doped IRMOF-8						
Parameters from	**X**	**Interaction Equation**	$r_{H\text{-}X}$ **(Å)**	$D_{H\text{-}X}/k_B$ **(K)**	$\alpha_{H\text{-}X}$ **(Å^{-1})**	**Partial charge**
This work, bare Li^+	Li^+	S2	2.017	1101.428	8.147	N/A
This work, $Li^+(C_{10}H_8)^-$	Li^+	S2	2.123	562.775	6.664	N/A
Deng *et al.*[6]	Li^+	S2	2.066	1361.751	6.684	N/A
Li Alkoxide-Functionalized IRMOF-8						
Parameters from	**X**	**Interaction Equation**	$r_{H\text{-}X}$ **or** $\sigma_{H2\text{-}X}$ **(Å)**	$D_{H\text{-}X}/k_B$ **or** $\varepsilon_{H2\text{-}X}/k_B$ **(K)**	$\alpha_{H\text{-}X}$ **(Å^{-1})**	**Partial charge**
Getman *et al.*[4]	Li^+	S3	2.271	226.993	2.086	+0.9
	O^-	S3	4.550	11.992	1.074	−0.9
Klontzas *et al.*[7]	Li^+	S4	1.80	1505.0	N/A	N/A
	O^-	S4	2.43	859.0	N/A	N/A

S1.4 Force Field Parameterization Procedure

Our force field parameterization procedure is described in depth in the Supporting Information of Ref.[4] The main points are summarized here.

S1.4.1 H_2/Li^+

Parameters for H_2 interactions with a bare Li^+ cation were obtained by fitting a Morse equation (Eq. S2) to discrete energies calculated using the Gaussian 09[8] quantum chemical software. We included two routes for H_2 to Li^+, one where H_2 binds side on to Li^+ and one where it binds head on. We allowed the H—H bond to relax in the calculations, but we held the H_2—Li^+ distance fixed at each point. Calculations were performed at the MP2/6-311+G** level of theory using the counterpoise method[9] to offset errors due to basis set superposition. The final set of parameters is given in Table S2. Force field energies are compared with *ab initio* energies in Figure S1. The RMS difference between force field and *ab initio* energies is 3.29 kJ mol^{-1} for all configurations where the *ab initio* energies are less than 0.

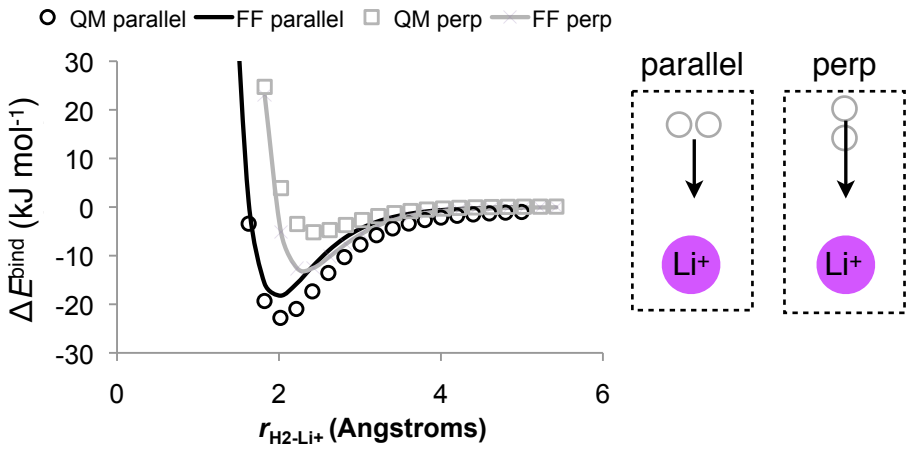

Figure S1. Interaction energies calculated with the Morse potential (Eq. S2, lines) compared with energies calculated with MP2/6-311+G** (symbols) for H_2 interactions with a bare Li^+cation.

S1.4.2 $H_2/Li^+(C_{10}H_8)^-$

Parameters for H_2 interactions with the Li ion in $Li^+(C_{10}H_8)^-$ were obtained by fitting a Morse + Lennard-Jones potential to discrete energies calculated using the Gaussian 09[8] quantum chemical software. The Morse and Lennard-Jones equations are given in Eqs. S2 and S4, respectively. In the quantum chemical calculations, the geometry of the $Li^+(C_{10}H_8)^-$ group was held fixed at the calculated optimum in the absence of H_2, the distance between the H_2 center of mass and Li^+ was held fixed at each point, and the orientation of the H_2 molecule was held fixed with respect to $Li^+(C_{10}H_8)^-$. The H—H bond was allowed to relax. We attempted to sample the entire interaction region surrounding Li^+, moving H_2 from 5 to 1.5 Å from Li^+ and exploring a variety of "approach" routes (see Figure S2). Calculations were performed at the MP2/6-311+G** level of theory using the counterpoise method[9] to offset errors due to basis set superposition. In these calculations, H_2, Li, and $C_{10}H_8$ were all considered to be separate fragments.

In the Morse + Lennard-Jones potential, dispersion and repulsion interactions between the H_2 center of mass and C and H were calculated with Lennard-Jones potentials, employing the parameters in Table S1 (these parameters were held fixed). Dispersion and repulsion interactions between each H nucleus and Li were calculated with a Morse potential. Morse parameters were obtained by fitting the pairwise sum of all interactions,

$$\mathcal{V}^{\text{force field}} = \sum_i \mathcal{V}_i^{\text{Morse}} + \sum_j \mathcal{V}_j^{\text{Lennard-Jones}} \qquad \text{(Eq. S5)}$$

where i is over the interactions between the H nuclei and Li, and j is over the interactions between the H_2 center of mass and the atoms in the $C_{10}H_8$ fragment, to the *ab initio* energies using a simulated annealing method.[10] The final set of parameters, i.e. the set that minimizes the root mean square difference between parameterized and *ab initio* energies, is given in Table S2.

Force field energies are compared with *ab initio* energies in Figure S2. The RMS difference between force field and *ab initio* energies is 1.40 kJ mol^{-1} for all configurations where the *ab initio* energies are less than 0.

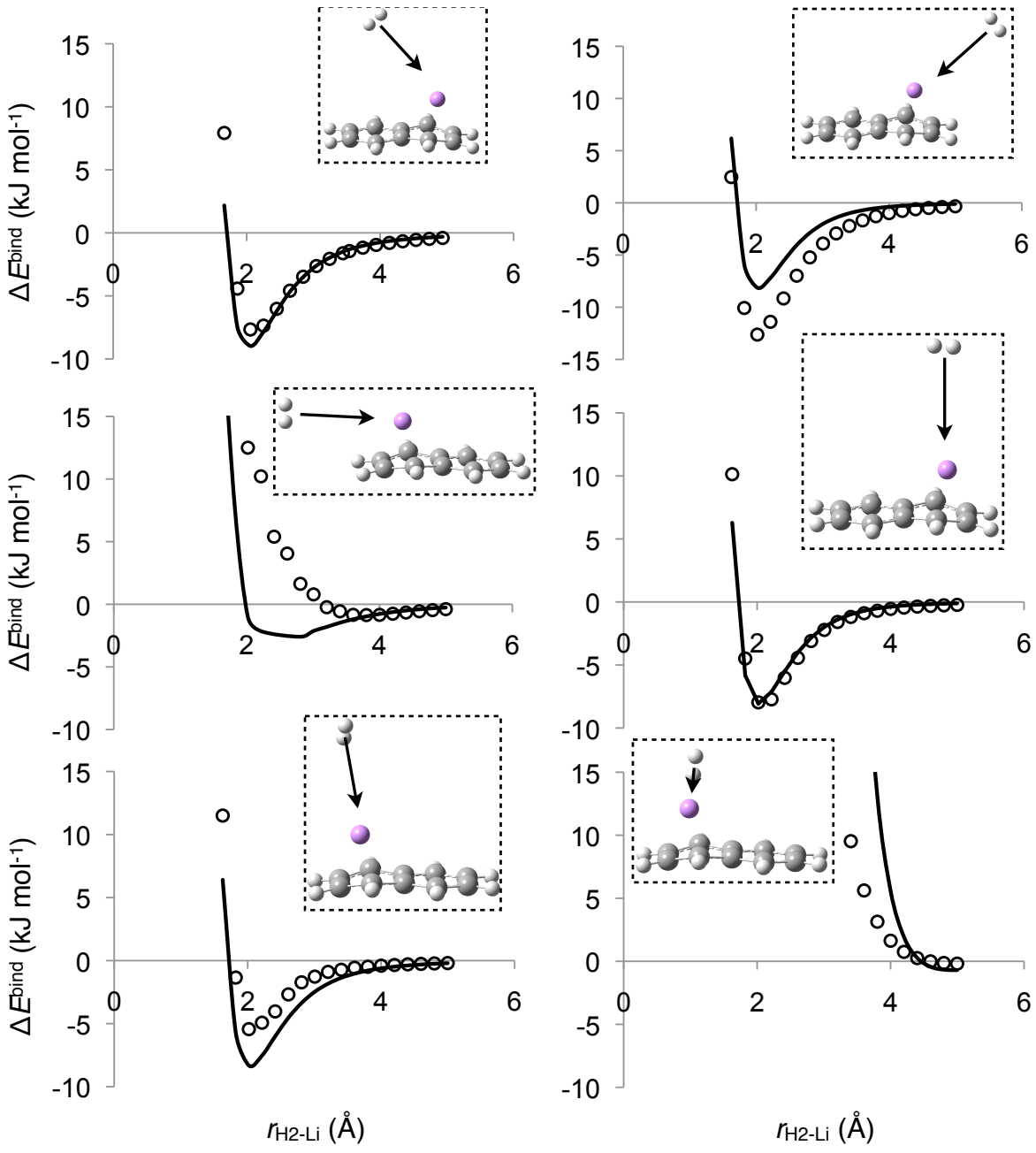

Figure S2. Interaction energies calculated with the Morse potential (Eq. S2, lines) compared with energies calculated with MP2/6-311+G** (symbols) for H_2 interactions with $Li^+(C_{10}H_8)^-$.

S1.4.3 H_2/Li Alkoxide

The force field parameterization fitting procedure for this system is described in depth in the Supporting Information of Ref.[4] The final set of parameters is given in Table S2. Force field energies are compared with *ab initio* energies in Figure S3. The RMS difference between force field and *ab initio* energies is 0.73 kJ mol^{-1} for all configurations where the *ab initio* energies are less than 0.

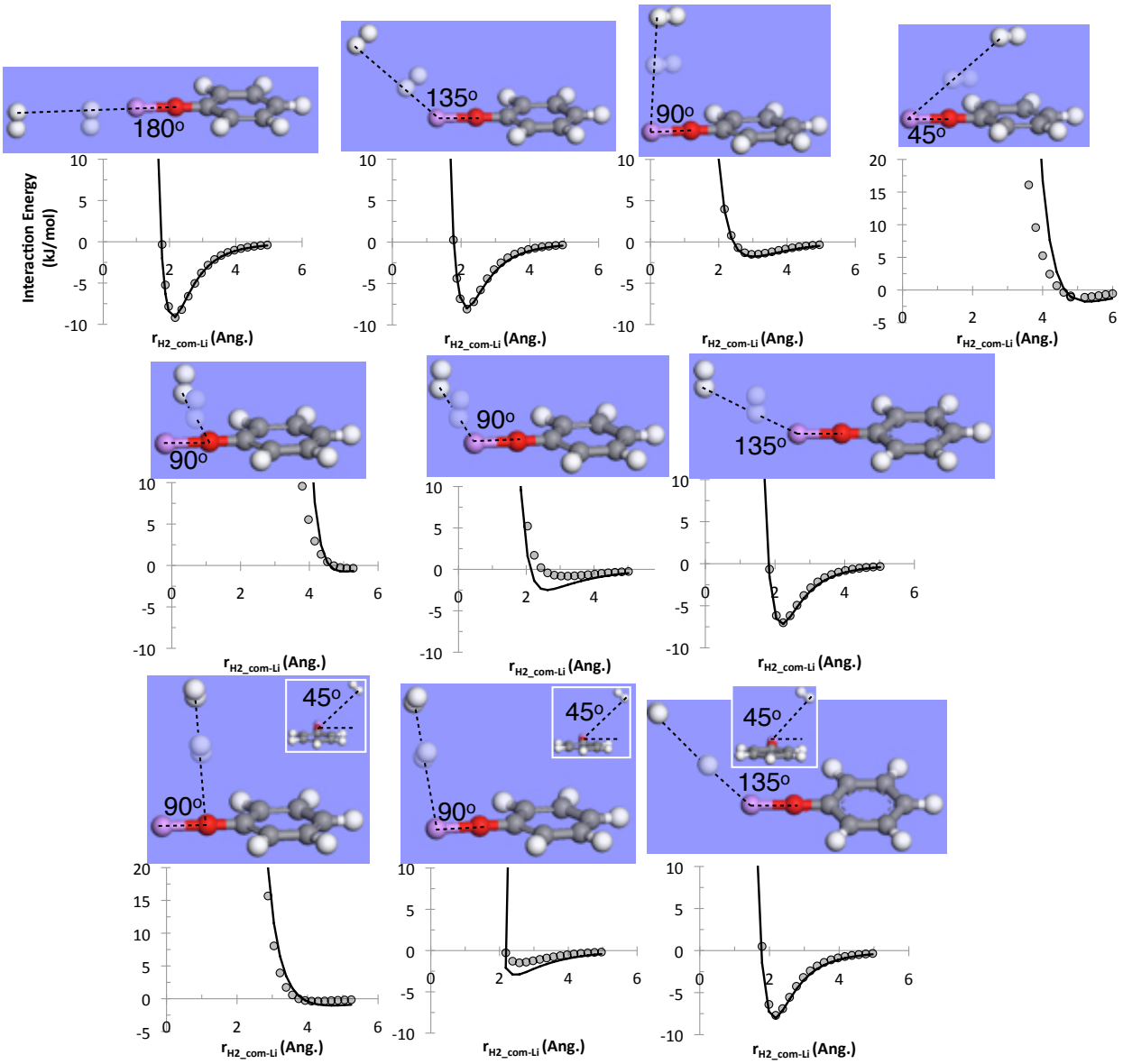

Figure S3. Interaction energies calculated with the modified-Morse/Lennard-Jones plus Coulomb potential described in Ref.[4] (lines) compared with energies calculated with MP2/6-311+G** (circles) for H_2 interaction with Li alkoxide benzene. In addition to the approaches shown here, we also sampled configurations with different H_2 configurations, such as "head on" adsorption to Li, for a total of 225 quantum chemical energies. Reproduced with permission from Getman *et al.*[4] Copyright 2011 American Chemical Society.

S2 H_2 Adsorption Simulations

Classical simulations were performed with our in-house, multipurpose code RASPA.[11] Positions of framework atoms were taken from crystallography[12]. Positions of Li (doped IRMOF-8) and

Li alkoxide groups (functionalized IRMOF-8) are not available from crystallography. These were taken from the *ab initio* calculations discussed above. The H_2 molecule was assumed to be rigid with a bond length of 0.741 Å. H_2/framework atom interactions were using the potentials and parameters described above. H_2 adsorption isotherms were calculated using grand canonical Monte Carlo (GCMC) simulations. In these simulations, 100,000 cycles were performed to equilibrate the positions of H_2 in the systems, and an additional 60,000 cycles were performed to compute ensemble averages. In each cycle, an average of N moves were performed, where N is the number of molecules in the system (which fluctuates in GCMC). GCMC moves used were translation, rotation, insertion, deletion, and reinsertion into a new position within the framework.

The isosteric heats of adsorption were computed from the GCMC simulations using the expression[13]

$$Q_{\mathrm{st}} = RT - \left(\frac{\partial \langle \mathcal{V} \rangle \langle N \rangle}{\partial \langle N \rangle} \right)_{T,V} \qquad \text{(Eq. S6)}$$

S3 Comparison of Simulated and Experimental Isotherms for CH_4 and H_2 Adsorption in MOFs

Table S3. Potential models used in GCMC simulations from the literature for CH_4 adsorption in MOFs and COFs and the agreement of the calculated isotherms with experiment

Literature	MOFs	T P_{max}	CH_4 model	MOF model	Expt Data	Agreement with expt.[a]
Düren et al.[14]	IRMOF-1 IRMOF-6	298 K 40 bar	spherical LJ[15]	DREIDING	16	good
Gallo and Glossman-Mitnik[17]	IRMOF-1	298 K 80 bar	spherical LJ[15]	UFF	16	good
Garberoglio et al.[18]	HKUST-1	295 K 1 bar	spherical LJ[19]	DREIDING or UFF	20	slightly +
Yang and Zhong[21]	IRMOF-1	298 K 40 bar	spherical LJ[22]	refitted portions of OPLS-AA	16	good
Yang and Zhong[23]	HKUST-1	295 K 1 bar	spherical LJ[22]	refitted portions of OPLS-AA	20	good
Wang[24]	$Cu(SiF_6)(bpy)_2$ $Cu(GeF_6)(bpy)_2$ CPL-2	298 K 35 bar	spherical LJ[22]	refitted portions of OPLS-AA	24-26	good
Lan et al.[25]	COF-102	298 K 100 bar	spherical LJ[15]	CH_4-MOF FFs from ab initio MP2 calculations	26	slightly +
Mendoza-Cortes et al.[27]	COF-5 COF-8	298 K 100 bar	CH_4-CH_4 FFs from ab initio MP2 calculations	CH_4-MOF FFs from ab initio MP2 calculations	27	good

[a]+: simulations overestimated experiments

Table S4. Potential models used in GCMC simulations from the literature for H_2 adsorption in MOFs and the agreement of the calculated isotherms with experiment

Literature	MOFs	T P_{max}	H_2 model[a] + Quantum diffraction effect[b]	MOF model	Expt Data	Agreement with expt.[c]
Frost et al.[28]	IRMOF-1 IRMOF-8	77 K 1 bar	spherical LJ[29]	DREIDING	12	− (low P) + (high P)
	IRMOF-18	77 K 1 bar	spherical LJ[29]	DREIDING	12	+
Frost et al.[30]	IRMOF-1	298 K 120 bar	spherical LJ[29]	DREIDING +UFF(Cu)	31-33	good (low P) − (high P)
	HKUST-1	298 K 120 bar	spherical LJ[29]	DREIDING +UFF(Cu)	31	good (low P) − (high P)
Ryan et al.[3]	IRMOF-1	77 K 298 K 120 bar	spherical LJ[29]	DREIDING	34	good
Gallo and Glossman-Mitnik[17]	IRMOF-1 IRMOF-11 MOF-74	298 K 80~100 bar	spherical LJ	UFF	35	good
Yang and Zhong[36]	IRMOF-1 IRMOF-18	77 K 1 bar	two-site LJ	refitted portions of OPLS-AA	12	good
Jung et al.[37]	IRMOF-1 IRMOF-18	77 K 1 bar	two-site LJ[36]	refitted portions of UFF	12,38	good
Jung et al.[39]	IRMOF-9	77 K 1 bar	two-site-LJ[36]	modified UFF[37]	40	+
	IRMOF-11	77 K 1 bar	two-site-LJ[36]	modified UFF[37]	12	good
	IRMOF-13	77 K 1 bar	two-site-LJ[36]	modified UFF[37]	40	slightly −
Sagara et al.[41]	IRMOF-1	78 K 1 bar	modified three-site (DL)	modified UFF	12	+
	IRMOF-1	298 K 50 bar	three- site	UFF	42,43	−
Yang and Zhong[44]	MOF-505	77 K 1 bar	three- site (DL)[5]	Refitted portions of OPLS-AA	45	good
Gaberoglio et al.[18]	Manganese formate	78 K 1 bar	three- site (DL)[5]	UFF or DREIDING	46	−
Gaberoglio et al.[18]	IRMOF-1	77 K 1 bar	spherical LJ (Buch)[47]	UFF	12	good
			spherical LJ (Buch)[47] + PIMC	UFF	12	good
			three- site (DL)[5]	UFF	12	+
Gaberoglio et al.[18]	IRMOF-8	77 K 1 bar	spherical LJ (Buch)[47]	UFF	12	− (low P)
			spherical LJ	UFF	12	− (low P)

			(Buch)[47] + PIMC			
Gaberoglio et al.[18]	IRMOF-1	298 K 95 bar	spherical LJ (Buch)[47]	UFF	42	–
			three- site (DL)[5]	UFF	42	–
	Cu-MMOM	298 K 45 bar	spherical LJ (Buch)[47]	UFF	43	–
Liu et al.[48]	HKUST-1	77 K 50 bar	spherical LJ (Buch)[47]	UFF	48	− (low P) slightly + (high P)
			spherical LJ (Buch)[47] + FH	UFF	48	– (low P) slightly − (high P)
	HKUST-1	87 K 50 bar	spherical LJ (Buch)[47] + FH	UFF	48	–
	HKUST-1	175 K 298 K 50 bar	spherical LJ (Buch)[47]	UFF	48	slightly − (175 K) good (298 K)
Liu et al.[49]	$Zn(bdc)(ted)_{0.5}$	77 K 50 bar	spherical LJ (Buch)[47] + FH	UFF	49	slightly + (low P)
			spherical LJ (Buch)[47] + FH	DREIDING	49	good
	$Zn(bdc)(ted)_{0.5}$	298 K 50 bar	spherical LJ (Buch)[47]	UFF	49	slightly +
			spherical LJ (Buch)[47]	DREIDING	49	good
Han et al.[50]	IRMOF-1	77 K 1 bar	FFs from ab initio second-order MP2 calculations		12	good

[a]Three-site model: three point charges with single LJ core
[b]FH: Feynman-Hibbs effective potential method[51]; PIMC: Path Integral Monte Carlo method[52]; if nothing is indicated, the simulations did not account for quantum diffraction effects
[c]+: simulations overestimated experiments; − : simulations underestimated experiments

References

(1) Mayo, S. L.; Olafson, B. D.; Goddard, W. A. *Journal of Physical Chemistry* **1990**, *94*, 8897.
(2) Michels, A.; Degraaff, W.; Tenseldam, C. A. *Physica* **1960**, *26*, 393.
(3) Ryan, P.; Broadbelt, L. J.; Snurr, R. Q. *Chem. Comm.* **2008**, 4132-4134.
(4) Getman, R. B.; Miller, J. H.; Wang, K.; Snurr, R. Q. *J. Phys. Chem. C* **2011**, *115*, 2066-2075.
(5) Darkrim, F.; Levesque, D. *Journal of Chemical Physics* **1998**, *109*, 4981-4984.
(6) Deng, W.-Q.; Xu, X.; Goddard, W. A. *Phys. Rev. Lett.* **2004**, *92*, 166103.
(7) Klontzas, E.; Tylianakis, E.; Froudakis, G. E. *J. Phys. Chem. C* **2009**, *113*, 21253.
(8) Frisch, M. J.; Trucks, G. W.; Schlegel, H. B.; Scuseria, G. E.; Robb, M. A.; Cheeseman, J. R.; Scalmani, G.; Barone, V.; Mennucci, B.; Petersson, G. A.; Nakatsuji, H.; Caricato,

M.; Li, X.; Hratchian, H. P.; Izmaylov, A. F.; Bloino, J.; Zheng, G.; Sonnenberg, J. L.; Hada, M.; Ehara, M.; Toyota, K.; Fukuda, R.; Hasegawa, J.; Ishida, M.; Nakajima, T.; Honda, Y.; Kitao, O.; Nakai, H.; Vreven, T.; J. A. Montgomery, J.; Peralta, J. E.; Ogliaro, F.; Bearpark, M.; Heyd, J. J.; Brothers, E.; Kudin, K. N.; Staroverov, V. N.; Kobayashi, R.; Normand, J.; Raghavachari, K.; Rendell, A.; Burant, J. C.; Iyengar, S. S.; Tomasi, J.; Cossi, M.; Rega, N.; Millam, J. M.; Klene, M.; Knox, J. E.; Cross, J. B.; Bakken, V.; Adamo, C.; Jaramillo, J.; Gomperts, R.; Stratmann, R. E.; Yazyev, O.; Austin, A. J.; Cammi, R.; Pomelli, C.; Ochterski, J. W.; Martin, R. L.; Morokuma, K.; Zakrzewski, V. G.; Voth, G. A.; Salvador, P.; Dannenberg, J. J.; Dapprich, S.; Daniels, A. D.; Farkas, O.; Foresman, J. B.; Ortiz, J. V.; Cioslowski, J.; Fox, D. J.; Revision A.02 ed.; Gaussian, Inc: Wallingford, CT, 2009.

(9) Boys, S. F.; Bernardi, F. *Mol. Phys.* **2002**, *100*, 65.

(10) Hayes, J. M.; Greer, J. C. *Comput. Phys. Commun.* **2002**, *147*, 803.

(11) Dubbeldam, D.; Calero, S.; Ellis, D. E.; Snurr, R. Q.; 1.0 ed.; Northwestern University: Evanston, IL, 2008.

(12) Rowsell, J. L.; Millward, A. R.; Park, K. S.; Yaghi, O. M. *J. Am. Chem. Soc.* **2004**, *126*, 5666.

(13) Snurr, R. Q.; Bell, A. T.; Theodorou, D. N. *J. Phys. Chem.* **1993**, *97*, 13742.

(14) Düren, T.; Sarkisov, L.; Yaghi, O. M.; Snurr, R. Q. *Langmuir* **2004**, *20*, 2683-2689.

(15) Goodbody, S. J.; Watanabe, K.; Macgowan, D.; Walton, J.; Quirke, N. *J. Chem. Soc. Farad. Trans.* **1991**, *87*, 1951.

(16) Eddaoudi, M.; Kim, J.; Rosi, N.; Vodak, D.; Wachter, J.; O'Keeffe, M.; Yaghi, O. M. *Science* **2002**, *295*, 469.

(17) Gallo, M.; Glossman-Mitnik, D. *J. Phys. Chem. C* **2009**, *113*, 6634-6642.

(18) Garberoglio, G.; Skoulidas, A. I.; Johnson, J. K. *J. Phys. Chem. B* **2005**, *109*, 13094-13103.

(19) Jiang, S. Y.; Gubbins, K. E.; Zollweg, J. A. *Molecular Physics* **1993**, *80*, 103-116.

(20) Wang, Q. M.; Shen, D. M.; Bulow, M.; Lau, M. L.; Deng, S. G.; Fitch, F. R.; Lemcoff, N. O.; Semanscin, J. *Microporous and Mesoporous Materials* **2002**, *55*, 217-230.

(21) Yang, Q. Y.; Zhong, C. L. *J. Phys. Chem. B* **2006**, *110*, 17776.

(22) Martin, M. G.; Siepmann, J. I. *J. Phys. Chem. B* **1998**, *102*, 2569-2577.

(23) Yang, Q. Y.; Zhong, C. L. *ChemPhysChem* **2006**, *7*, 1417.

(24) Wang, S. Y. *Energy & Fuels* **2007**, *21*, 953-956.

(25) Lan, J. H.; Cao, D. P.; Wang, W. C. *Langmuir* **2009**, *26*, 220-226.

(26) Furukawa, H.; Yaghi, O. M. *Journal of the American Chemical Society* **2009**, *131*, 8875-8883.

(27) Mendoza-Cortes, J. L.; Han, S. S.; Furukawa, H.; Yaghi, O. M.; Goddard, W. A. *Journal of Physical Chemistry A* **2010**, *114*, 10824-10833.

(28) Frost, H.; Düren, T.; Snurr, R. Q. *J. Phys. Chem. B* **2006**, *110*, 9565.

(29) Michels, A.; Degraaff, W.; Tenseldam, C. A. *Physica* **1960**, *26*, 393.

(30) Frost, H.; Snurr, R. Q. *Journal of Physical Chemistry C* **2007**, *111*, 18794.

(31) Panella, B.; Hirscher, M.; Putter, H.; Muller, U. *Advanced Functional Materials* **2006**, *16*, 520-524.

(32) Poirier, E.; Chahine, R.; Benard, P.; Lafi, L.; Dorval-Douville, G.; Chandonia, P. A. *Langmuir* **2006**, *22*, 8784-8789.

(33) Li, Y. W.; Yang, R. T. *Journal of the American Chemical Society* **2006**, *128*, 8136-8137.

(34) Kaye, S. S.; Dailly, A.; Yaghi, O. M.; Long, J. R. *Journal of the American Chemical Society* **2007**, *129*, 14176-14177.
(35) Rowsell, J. L. C. Ph.D. Dissertation, University of Michigan, 2005.
(36) Yang, Q. Y.; Zhong, C. L. *Journal of Physical Chemistry B* **2005**, *109*, 11862-11864.
(37) Jung, D. H.; Kim, D.; Lee, T. B.; Kim, J.; Choi, S. H. In *Advances in Nanomaterials and Processing, Pts 1 and 2*; Ahn, B. T., Jeon, H., Hur, B. Y., Kim, K., Park, J. W., Eds.; Trans Tech Publications Ltd: Stafa-Zurich, 2007; Vol. 124-126.
(38) Kim, D.; Lee, T. B.; Choi, S. B.; Yoon, J. H.; Kim, J.; Choi, S. H. *Chemical Physics Letters* **2006**, *420*, 256-260.
(39) Jung, D. H.; Kim, D.; Lee, T. B.; Choi, S. B.; Yoon, J. H.; Kim, J.; Choi, K.; Choi, S. H. *Journal of Physical Chemistry B* **2006**, *110*, 22987-22990.
(40) Rowsell, J. L. C.; Yaghi, O. M. *J. Am. Chem. Soc.* **2006**, *128*, 1304-1315.
(41) Sagara, T.; Klassen, J.; Ganz, E. *Journal of Chemical Physics* **2004**, *121*, 12543.
(42) Rosi, N. L.; Eckert, J.; Eddaoudi, M.; Vodak, D. T.; Kim, J.; O'Keeffe, M.; Yaghi, O. M. *Science* **2003**, *300*, 1127-1129.
(43) Pan, L.; Sander, M. B.; Huang, X. Y.; Li, J.; Smith, M.; Bittner, E.; Bockrath, B.; Johnson, J. K. *Journal of the American Chemical Society* **2004**, *126*, 1308-1309.
(44) Yang, Q. Y.; Zhong, C. L. *J. Phys. Chem. B* **2006**, *110*, 655-658.
(45) Chen, B. L.; Ockwig, N. W.; Millward, A. R.; Contreras, D. S.; Yaghi, O. M. *Angewandte Chemie-International Edition* **2005**, *44*, 4745.
(46) Dybtsev, D. N.; Chun, H.; Yoon, S. H.; Kim, D.; Kim, K. *J. Am. Chem. Soc.* **2004**, *126*, 32-33.
(47) Buch, V. *Journal of Chemical Physics* **1994**, *100*, 7610-7629.
(48) Liu, J. C.; Culp, J. T.; Natesakhawat, S.; Bockrath, B. C.; Zande, B.; Sankar, S. G.; Garberoglio, G.; Johnson, J. K. *Journal of Physical Chemistry C* **2007**, *111*, 9305-9313.
(49) Liu, J.; Lee, J. Y.; Pan, L.; Obermyer, R. T.; Simizu, S.; Zande, B.; Li, J.; Sankar, S. G.; Johnson, J. K. *J. Phys. Chem. C* **2008**, *112*, 2911-2917.
(50) Han, S. S.; Deng, W. Q.; Goddard, W. A. *Angewandte Chemie-International Edition* **2007**, *46*, 6289-6292.
(51) Feynman, R. P.; Hibbs, A. R. *Quantum Mechanics and Path Integrals*; McGraw-Hill: New York, 1965.
(52) Feynman, R. P. *Reviews of Modern Physics* **1948**, *20*, 367-387.